Phase Noise in Coupled Oscillators: Theory and Experiment

Heng-Chia Chang, Xudong Cao, Umesh K. Mishra, *Fellow, IEEE,* and Robert A. York, *Member, IEEE*

***Abstract*—Phase noise in mutually synchronized oscillator systems is analyzed for arbitrary coupling and injection-locking topologies, neglecting amplitude noise, and amplitude modulation (AM) to phase modulation (PM) conversion. When the coupling phase is chosen properly (depending on the oscillator model), the near-carrier phase noise is reduced to $1/N$ that of a single oscillator, provided the coupling network is reciprocal. This is proved in general, and illustrated with specific cases of globally coupled and nearest-neighbor coupled oscillator chains. A slight noise degradation is found for unilaterally coupled (nonreciprocal) chains. The $1/N$ reduction for reciprocal coupling applies over nearly the entire range of free-running frequency distributions required for beam-scanning, and is verified experimentally using a linear chain of coupled GaAs MESFET voltage-controlled oscillators (VCO's) operating at *X*-band. The effect of a nonoptimum coupling phase on the phase noise of the system is also studied. As the coupling phase deviates from the optimum value, the phase noise increases significantly near the locking range edge for noise offset frequency near the carrier.**

***Index Terms*—AM noise, coupling topology, noise admittance, oscillators, phase noise, power spectral density.**

I. Introduction

COUPLED oscillator systems possess synchronization properties that may be suitable for certain millimeter-wave power-combining and beam-scanning applications [1]–[4]. In previous analytical and experimental work it has been shown that robust locking favors a low-Q oscillator design, which implies a large locking range. Unfortunately, low Q-factors also imply larger phase noise. Military applications for millimeter-wave sources in compact radar or communications systems may require better than -120 dBC/Hz noise-to-carrier ratio at 10 kHz offset. Similarly, commercial digital communication systems place strict constraints on the signal-to-noise ratio and the bit error rate (BER) for high-fidelity transmission [5], [7]. In this paper, the authors show that the total phase noise of the array is significantly reduced compared to that of a single free-running element in the array in direct proportion to the number of array elements, provided the coupling network is designed properly. For typical microwave FET oscillators, this result persists even when the oscillators are detuned with respect to each other, until the detuning is so large as to preclude mutual synchronization, at which point the phase fluctuations return to their free-running values.

This analysis extends the authors' prior work in coupled-oscillator theory to include a noisy Van der Pol oscillator. This is done by using a complex *noise admittance*, first suggested in [8], [9], which conveniently models the complexities [12] of a typical oscillator. The resulting dynamic equations describing the amplitude and phase fluctuations of the oscillators closely resemble the authors' prior (noiseless) work, and apply to arbitrary broad-band coupling networks [13]. In the general case, the equations describe the transformation of amplitude-modulation (AM) and phase-modulation (PM) noise from the noise admittance terms—corresponding to the real and imaginary parts of the noise admittance, respectively, to the individual oscillator output fluctuations. The equations cannot be solved analytically. However, restricting attention to phase noise and neglecting AM-to-PM conversion terms in the analysis permits an analytical solution for simple coupling networks, which accurately describes near-carrier noise for many cases of practical interest.

Specific N-element oscillator chains considered in this paper are shown in Fig. 1, including global coupling and nearest-neighbor coupling (bilateral and unilateral) configurations. In each case, it is assumed that the independent noise sources of the oscillators are mutually uncorrelated but generate identical power spectra. The globally coupled situation of Fig. 1(a) is analogous to the single-cavity multiple device oscillator [14], and is treated here primarily as a means for comparing the results against previously published literature [8]–[10], [14]. The nearest-neighbor bilateral and unilateral coupling topologies are relevant to recently proposed power combining and beam-scanning applications [2], [3]. For all *reciprocal* coupling topologies, it will be shown that the total phase noise is reduced in proportion to $1/N$, provided the coupling phase is chosen correctly. As the coupling phase deviates from this optimum value, the phase noise can increase significantly near the locking range edge, depending on the offset frequency from the carrier. The results are verified experimentally using a linear chain of coupled GaAs MESFET voltage-controlled oscillators (VCO's) operating at X-band.

II. Coupled Oscillator Noise Theory

A. Noisy Oscillator Model and Array Dynamics

Previous work has demonstrated the utility of a simple single-resonance negative-resistance oscillator model for array

Manuscript received June 3, 1996; revised January 24, 1997. This work was supported by the Hughes Research Laboratory and the Army Research Office.

The authors are with the Department of Electrical and Computer Engineering, University of California at Santa Barbara, Santa Barbara, CA 93106 USA.

Publisher Item Identifier S 0018-9480(97)02895-0.

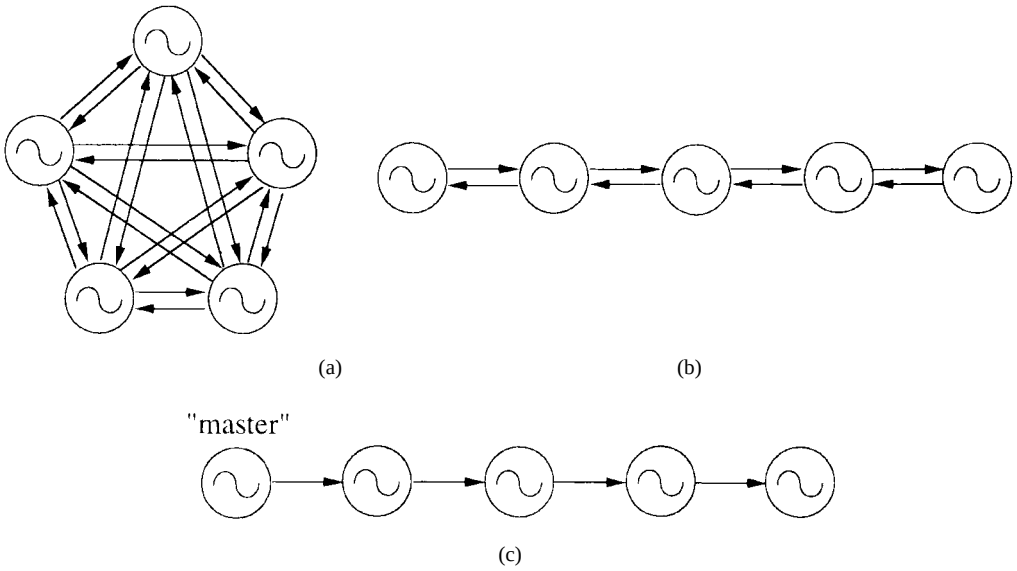

Fig. 1. Coupling topologies considered in this paper (illustrated for a five-oscillator system). (a) Global coupling. (b) Nearest-neighbor bilateral coupling. (c) Nearest-neighbor unilateral coupling.

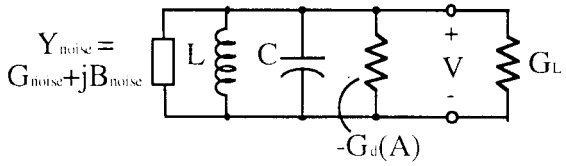

Fig. 2. Parallel negative-conductance oscillator model with a complex noise admittance.

analysis. This model is capable of generating all of the observed synchronization phenomenon. Either a series or parallel circuit is used, depending on the device characteristics; if the device is best modeled as a negative resistance, a series circuit is employed. If the device is best modeled as a negative conductance, a parallel model is employed, as shown in Fig. 2. Both models lead to similar synchronization properties. Noisy oscillators can be modeled either through the addition of an equivalent noise–current generator, or with an equivalent noise admittance $Y_{\text{noise}} = G_{\text{noise}} + jB_{\text{noise}}$ as shown in Fig. 2. It is convenient to define a normalized admittance $Y_n = G_n + jB_n$ with $G_n = G_{\text{noise}}/G_L$ and $B_n = B_{\text{noise}}/G_L$, where the normalization variable G_L parameter is the oscillator load admittance in the free-running state.

The terms G_n and B_n describe the in-phase and quadrature component of the noise signal, respectively. For the single oscillator case it will be shown that G_n physically corresponds to the oscillator amplitude fluctuations, while B_n corresponds to the phase fluctuations. For two or more coupled oscillators, the nonlinear interaction gives rise to cross coupling between the two types of noise. Use of the noise admittance obviates a detailed description of the noise statistics and physical origin, which is a useful simplification here since only a relative comparison of total-array phase noise with that of the individual oscillator is desired.

The oscillators are coupled through an arbitrary N-port network that is described by Y-parameters [13]. Once the oscillator model has been specified as above, the dynamic equations for amplitude and phase of each oscillator are determined in a straightforward manner [13] giving

$$\frac{\partial A_i}{\partial t} = \frac{\mu\omega_i}{2Q}(\alpha_i^2 - A_i^2)A_i + \frac{\omega_i}{2Q}\sum_{j=1}^{N}\epsilon_{ij}A_j \cdot \cos(\theta_i - \theta_j + \Phi_{ij}) - \frac{\omega_i}{2Q}A_i G_{ni}(t) \tag{1}$$

$$\frac{\partial \theta_i}{\partial t} = \omega_i - \frac{\omega_i}{2Q}\sum_{j=1}^{N}\frac{\epsilon_{ij}A_j}{A_i}\sin(\theta_i - \theta_j + \Phi_{ij}) - \frac{\omega_i}{2Q}B_{ni}(t) \tag{2}$$

where A_i, θ_i, ω_i, and Q are the amplitude, phase, free-running frequency, and Q-factor of the ith oscillator, respectively, and ϵ_{ij} and Φ_{ij} are the coupling parameters between the ith and jth oscillators. These nonlinear coupled equations cannot be solved analytically without approximation.

B. Solution for Phase Fluctuations

For noise analysis, the equations are perturbed by substituting $A_i \Rightarrow \hat{A}_i + \delta A_i$ and $\theta_i \Rightarrow \hat{\theta}_i + \delta\theta_i$ where $(\hat{A}, \hat{\theta})$ are the steady-state solutions to (1) and (2), and $(\delta A_i, \delta\theta_i)$ are the amplitude and phase fluctuations of the ith oscillator, respectively. Assuming small fluctuations, the equations can be linearized around $(\hat{A}, \hat{\theta})$ and become

$$\frac{\partial \delta A_i}{\partial t} = \mu\omega_{3\,\text{dB}}(\alpha_i^2 - 3\hat{A}_i^2)\delta A_i + \omega_{3\,\text{dB}}\sum_{j=1}^{N}\delta A_j\epsilon_{ij} \cdot \cos(\hat{\theta}_i - \hat{\theta}_j + \Phi_{ij}) - \omega_{3\,\text{dB}}\sum_{j=1}^{N}\epsilon_{ij}(\delta\theta_i - \delta\theta_j) \cdot \hat{A}_j \sin(\hat{\theta}_i - \hat{\theta}_j + \Phi_{ij}) - \omega_{3\,\text{dB}}\hat{A}_i G_{ni}(t) \tag{3}$$

$$\frac{\partial \delta\theta_i}{\partial t} = -\omega_{3\,\mathrm{dB}} \sum_{j=1}^{N} \frac{\epsilon_{ij}\hat{A}_j}{\hat{A}_i} \frac{\delta A_j - \delta A_i}{\hat{A}_i} \sin(\hat{\theta}_i - \hat{\theta}_j + \Phi_{ij}) - \omega_{3\,\mathrm{dB}} \sum_{j=1}^{N} \epsilon_{ij}(\delta\theta_i - \delta\theta_j) \frac{\hat{A}_j}{\hat{A}_i} \cos(\hat{\theta}_i - \hat{\theta}_j + \Phi_{ij}) - \omega_{3\,\mathrm{dB}} B_{ni}(t) \tag{4}$$

where $\omega_{3\,\mathrm{dB}} \equiv \omega_i/2Q$, half the 3-dB bandwidth of the oscillator tank circuits (assumed identical to first order).

In previous papers [1], [13], the authors have shown that it is desirable to operate the array using a coupling network designed to give $\Phi_{ij} = 2\pi$, so that for identical oscillators and free-running frequencies the stable locked state has all oscillators in-phase. This will be assumed to be the case here. Also, the spectral characteristics of the noise fluctuations are of most interest. Fourier transforming (3) and (4) gives

$$\left(\frac{j\omega}{\omega_{3\,\mathrm{dB}}}\right)\widetilde{\delta A}_i = \mu(\alpha_i^2 - 3\hat{A}_i^2)\widetilde{\delta A}_i + \sum_{j=1}^{N} \epsilon_{ij}\widetilde{\delta A}_j \cdot \cos(\hat{\theta}_i - \hat{\theta}_j) - \sum_{j=1}^{N} \epsilon_{ij}(\widetilde{\delta\theta}_i - \widetilde{\delta\theta}_j) \cdot \hat{A}_j \sin(\hat{\theta}_i - \hat{\theta}_j) - \hat{A}_i\tilde{G}_{ni} \tag{5}$$

$$\left(\frac{j\omega}{\omega_{3\,\mathrm{dB}}}\right)\widetilde{\delta\theta}_i = -\sum_{j=1}^{N} \frac{\epsilon_{ij}\hat{A}_j}{\hat{A}_i}\left(\frac{\widetilde{\delta A}_j - \widetilde{\delta A}_i}{\hat{A}_i}\right) \sin(\hat{\theta}_i - \hat{\theta}_j) - \sum_{j=1}^{N} \epsilon_{ij}(\widetilde{\delta\theta}_i - \widetilde{\delta\theta}_j) \frac{\hat{A}_j}{\hat{A}_i} \cos(\hat{\theta}_i - \hat{\theta}_j) - \tilde{B}_{ni} \tag{6}$$

where the tilde (˜) denotes a transformed or spectral variable, and ω is the noise frequency measured relative to the carrier. In (5), the second term of the right-hand side (RHS) represents the AM noise transformed from all the $j \neq i$ oscillators to the AM noise of the ith oscillator, and the third term represents conversion of PM noise to AM noise. Similarly in (6), the first term of the RHS represents AM noise transformed to PM noise, and the second term is PM-to-PM noise. Note that there is no mutual transformation between the AM noise and PM noise when the oscillators are in-phase, i.e., $\hat{\theta}_i = \hat{\theta}_j$ for all $i \neq j$. This result is consistent with that of [8] and [10].

One can write (5) and (6) in the following concise matrix format:

$$\begin{pmatrix} \mathrm{AM} \rightarrow \mathrm{AM} & \mathrm{PM} \rightarrow \mathrm{AM} \\ \mathrm{AM} \rightarrow \mathrm{PM} & \mathrm{PM} \rightarrow \mathrm{PM} \end{pmatrix} \begin{pmatrix} \overline{\widetilde{\delta A}} \\ \overline{\widetilde{\delta\theta}} \end{pmatrix} = \begin{pmatrix} \overline{\hat{A}\tilde{G}}_n \\ \overline{\tilde{B}}_n \end{pmatrix} \tag{7}$$

where $\overline{\hat{A}\tilde{G}}_n$ is the $N \times 1$ in-phase or AM noise-source vector, and $\overline{\tilde{B}}_n$ is the $N \times 1$ quadrature or PM noise-source vector. For simplicity, focus here will be on the PM-to-PM noise conversion, assuming all the steady-state amplitudes are identical. Under these assumptions, (6) reduces to

$$j\left(\frac{\omega}{\omega_{3\,\mathrm{dB}}}\right)\widetilde{\delta\theta}_i = -\sum_{j=1}^{N} \epsilon_{ij}(\widetilde{\delta\theta}_i - \widetilde{\delta\theta}_j) \cos(\hat{\theta}_i - \hat{\theta}_j) - \tilde{B}_{ni}, \quad i = 1 \cdots N. \tag{8}$$

The matrix form of (8) is

$$\overline{\overline{N}}\,\overline{\widetilde{\delta\theta}} = \overline{\tilde{B}}_n \tag{9}$$

where

$$\overline{\widetilde{\delta\theta}} = \begin{pmatrix} \widetilde{\delta\theta}_1 \\ \widetilde{\delta\theta}_2 \\ \vdots \\ \widetilde{\delta\theta}_N \end{pmatrix}, \qquad \overline{\tilde{B}}_n = \begin{pmatrix} \tilde{B}_{n1} \\ \tilde{B}_{n2} \\ \vdots \\ \tilde{B}_{nN} \end{pmatrix}.$$

The matrix $\overline{\overline{N}}$ will reflect the coupling topology of the N-element coupled oscillator array. The phase fluctuations of the individual oscillator are then determined by the matrix equation

$$\overline{\widetilde{\delta\theta}} = \overline{\overline{P}}\,\overline{\tilde{B}}_n \tag{10}$$

where $\overline{\overline{P}} = \overline{\overline{N}}^{-1}$. Since many of the coupling topologies possess some intrinsic symmetry which leads to common solutions for all of the phase fluctuations, it is useful to simplify (10) by writing

$$\widetilde{\delta\theta}_i = \sum_{j=1}^{N} p_{ij}\tilde{B}_{nj} \tag{11}$$

where p_{ij} is an element of the matrix $\overline{\overline{P}}$.

The power spectrum of the individual noise fluctuations is given by $\langle \widetilde{\delta\theta}_i \widetilde{\delta\theta}_i^* \rangle$, where the notation $\langle\ \rangle$ represents an ensemble average. Evaluating these power spectra using (11) leads to cross-power spectral densities of the form $\langle \tilde{B}_{nj}\tilde{B}_{nk}^* \rangle$. Assuming the quadrature noise sources, $B_{ni}(t)$, are random (ergodic) processes with zero time average, it can be shown using the Wiener–Khintchine theorem [11] that

$$\langle \tilde{B}_{ni}\tilde{B}_{nj}^* \rangle = \langle |\tilde{B}_{ni}|^2 \rangle \delta_{ij} \tag{12}$$

where δ_{ij} is the Kronecker delta. The term $\langle |\tilde{B}_{ni}|^2 \rangle$ is the power spectral density of the ith oscillator's quadrature noise source. It will be further assumed that all the oscillator noise sources have the same power spectral density, so that

$$\langle |\tilde{B}_{n1}|^2 \rangle = \langle |\tilde{B}_{n2}|^2 \rangle = \cdots = \langle |\tilde{B}_{nN}|^2 \rangle = \langle |\tilde{B}_n|^2 \rangle. \tag{13}$$

Furthermore, for notational convenience the notation $\langle\ \rangle$ will be hereafter dropped and the power spectrum will be written simply as $|\widetilde{\delta\theta}|^2$ or $|\tilde{B}_n|^2$, with the ensemble or time average being implicitly understood.

Using (12), one can write the power spectral density of the ith-oscillator phase fluctuation (i.e., the phase noise) as

$$|\widetilde{\delta\theta}_i|^2 = |\tilde{B}_n|^2 \sum_{j=1}^{N} |p_{ij}|^2 \tag{14}$$

which indicates that the ith element phase noise is found by summing the magnitude square of the elements in the ith *row* of the matrix $\overline{\overline{P}}$.

The combined output of all the array elements is the most important quantity of interest in coupled-oscillator array applications. Assuming the outputs are combined efficiently, the combined output signal is given by

$$V(t) = A \sum_{j=1}^{N} \cos(\omega_o t + \delta\theta_j) \tag{15}$$

where the oscillators are locked to a common frequency ω_o. Using the small fluctuation assumption allows (15) to be written as

$$V(t) = NA \cos(\omega_o t + \delta\theta_{\text{total}}) \tag{16}$$

where

$$\delta\theta_{\text{total}} = \frac{1}{N} \sum_{j=1}^{N} \delta\theta_j. \tag{17}$$

Using (11), one can write (17) as

$$\widetilde{\delta\theta}_{\text{total}} = \frac{1}{N} \sum_{j=1}^{N} \left(\sum_{i=1}^{N} p_{ij} \right) \tilde{B}_{nj}. \tag{18}$$

Again using (12), one can write the total phase noise as

$$|\widetilde{\delta\theta}_{\text{total}}|^2 = \frac{|\tilde{B}_n|^2}{N^2} \sum_{j=1}^{N} \left| \sum_{i=1}^{N} p_{ij} \right|^2 \tag{19}$$

which indicates that the total phase noise is found by summing the *columns* of the matrix $\overline{\overline{P}}$. Many of the commonly encountered coupling matrices have properties that make carrying out the indicated sums in both (14) and (19) straightforward.

C. Free-Running Oscillator Result

The noise properties of the N-coupled oscillators relative to a single free-running oscillator are desired. The noise properties of a single oscillator are found by setting $\epsilon = 0$ such that there is no mutual coupling between the oscillators. Then, (5) and (6) become

$$\left[\frac{\jmath\omega}{\omega_{3\,\text{dB}}} - \mu(\alpha_i^2 - 3\hat{A}_i^2) \right] \widetilde{\delta A}_i = -\hat{A}_i \tilde{G}_{ni} \tag{20}$$

and

$$\frac{\jmath\omega}{\omega_{3\,\text{dB}}} \widetilde{\delta\theta}_i = -\tilde{B}_{ni}. \tag{21}$$

Therefore, the AM noise for single oscillator is

$$|\widetilde{\delta A}_i|^2_{\text{uncoupled}} = \frac{\hat{A}_i^2 |\tilde{G}_{ni}|^2}{\left(\frac{\omega}{\omega_{3\,\text{dB}}} \right)^2 + \mu^2 (3\hat{A}_i^2 - \alpha_i^2)^2} \tag{22}$$

where α_i and $\hat{A}_i$ are the free-running oscillator amplitude, and the steady state amplitude after coupling, respectively. The PM noise of single oscillator is

$$|\widetilde{\delta\theta}_i|^2_{\text{uncoupled}} = \frac{|\tilde{B}_{ni}|^2}{\left(\frac{\omega}{\omega_{3\,\text{dB}}} \right)^2}. \tag{23}$$

These results have the same form as those in [15], [16]. Note that for most oscillators, noise close to the carrier ($\omega \ll \omega_{3\,\text{dB}}$) is dominated by phase noise. This somewhat justifies the neglect of amplitude noise and AM-to-PM conversion, even for nonuniform phase progressions. The result (23) features prominently in the following derivations.

III. Globally Coupled Oscillator Arrays

The validity of this formulation can be tested by comparing it to the globally coupled oscillator array (the completely coupled system [5]) which has been treated elsewhere [8]–[10], [14]. This case [illustrated in Fig. 1(a)] corresponds to a coupling coefficient $\epsilon_{ij} = \epsilon$ for any i and j. Assuming the oscillators are all in phase, (8) becomes

$$\jmath\omega\widetilde{\delta\theta}_i = \Delta\omega_{\text{lock}} \left[-(N-1)\widetilde{\delta\theta}_i + (\widetilde{\delta\theta}_1 + \widetilde{\delta\theta}_2 + \cdots + \widetilde{\delta\theta}_N) - \frac{1}{\varepsilon} \tilde{B}_{ni} \right] \tag{24}$$

where $\Delta\omega_{\text{lock}} = \epsilon\omega_{3\,\text{dB}}$ is half the total locking range [1]. Putting (24) in the matrix form (9) gives the PM-to-PM noise matrix for global coupling, as shown in (25) at the bottom of the page, where $x = \omega/\Delta\omega_{\text{lock}}$. The inverse matrix can be

$$\overline{\overline{N}} = \epsilon \begin{pmatrix} 1-N-\jmath x & 1 & 1 & \cdots & 1 \\ 1 & 1-N-\jmath x & 1 & \cdots & 1 \\ 1 & 1 & 1-N-\jmath x & \ddots & \vdots \\ \vdots & \vdots & \ddots & \ddots & 1 \\ 1 & 1 & \cdots & 1 & 1-N-\jmath x \end{pmatrix} \tag{25}$$

easily found for this case and is given by

$$\overline{\overline{P}} = \frac{1}{-\epsilon jx(N+jx)} \cdot \begin{pmatrix} 1+jx & 1 & 1 & \cdots & 1 \\ 1 & 1+jx & 1 & \cdots & 1 \\ 1 & 1 & 1+jx & \ddots & \vdots \\ \vdots & \vdots & \ddots & \ddots & 1 \\ 1 & 1 & \cdots & 1 & 1+jx \end{pmatrix}. \quad (26)$$

In this case it is clear that

$$\sum_{i=1}^{N} p_{ij} = \frac{-1}{j\epsilon x} = \frac{-1}{\frac{j\omega}{\omega_{3\,\mathrm{dB}}}}, \qquad \text{for all } j \quad (27)$$

so, from (17), the total output phase noise is

$$|\widetilde{\delta\theta}_{\mathrm{total}}|^2 = \frac{1}{N} \frac{|\tilde{B}_n|^2}{\left(\frac{\omega}{\omega_{3\,\mathrm{dB}}}\right)^2}. \quad (28)$$

Comparing (28) with the single-oscillator noise result in (23) we find

$$|\widetilde{\delta\theta}_{\mathrm{total}}|^2 = \frac{1}{N} \left|\widetilde{\delta\theta}_i\right|^2_{\mathrm{uncoupled}}. \quad (29)$$

The total PM noise for N globally coupled oscillators becomes $1/N$ of that of a single oscillator. This result agrees with [8]–[10], [14], and suggests that the mutual synchronization does not lead to any significant correlation of the oscillator phase fluctuations.

The noise property of the individual oscillators in the globally coupled array is also of interest. From (14) and (26) the power spectral density for the ith oscillator in the array is found as

$$|\widetilde{\delta\theta}_i|^2 = \frac{N + \left(\frac{\omega}{\Delta\omega_{\mathrm{lock}}}\right)^2}{N^2 + \left(\frac{\omega}{\Delta\omega_{\mathrm{lock}}}\right)^2} \left|\widetilde{\delta\theta}_i\right|^2_{\mathrm{uncoupled}}. \quad (30)$$

Again, the primary interest is with the phase noise near the carrier, so that $\omega \ll \Delta\omega_{\mathrm{lock}}$, in which case

$$|\widetilde{\delta\theta}_i|^2 \to \frac{1}{N} \left|\widetilde{\delta\theta}_i\right|^2_{\mathrm{uncoupled}}. \quad (31)$$

At the other extreme (far from the carrier), the individual oscillators approach the free-running noise properties

$$|\widetilde{\delta\theta}_i|^2 \to |\widetilde{\delta\theta}_i|^2_{\mathrm{uncoupled}}. \quad (32)$$

To summarize: after adding the coupling circuits, the individual oscillators and the total array output have a phase noise reduction near the carrier frequency in direct proportion to the number of oscillators, N. The PM noise of the individual oscillators far from the carrier frequency is not affected by the coupling circuits and still has the same noise properties as the original oscillator.

IV. Nearest-Neighbor Bilaterally Coupled Chains

A case of practical interest for microwave oscillator arrays is a nearest-neighbor mutually coupled coupled system, which is simple to construct and is known to possess desirable attributes for beam-scanning [1], [2], [13]. This case [shown in Fig. 1(b)] is described by the coupling parameters

$$\epsilon_{ij} = \begin{cases} \epsilon, & |i-j| = 1 \\ 0, & \text{otherwise} \end{cases} \quad (33)$$

where ϵ is a constant that can be related to the circuit design [13]. To keep the math tractable one will also assume a constant phase progression along the array so that $\hat{\theta}_i - \hat{\theta}_{i+1} = \Delta\hat{\theta}$. As described in the authors' previous papers [1], [2], this phase progression can be established by varying the free-running frequencies of both the end oscillators, while keeping the central elements at a common free-running frequency.

For this configuration the matrix $\overline{\overline{N}}$ in (9) is shown in (34) at the bottom of the page, where $x = \omega/(\Delta\omega_{\mathrm{lock}} \cos\Delta\hat{\theta})$. The inverse of $\overline{\overline{N}}$ is not easily expressed for the general case. However, note that from the relation $\overline{\overline{P}}\,\overline{\overline{N}} = \overline{\overline{N}}\,\overline{\overline{P}} = \overline{\overline{I}}$ one can write

$$\sum_{j=1}^{N} n_{ij} p_{jk} = \delta_{ik}$$
$$\sum_{i=1}^{N} \sum_{j=1}^{N} n_{ij} p_{jk} = \sum_{j=1}^{N} p_{jk} \left(\sum_{i=1}^{N} n_{ij}\right) = 1. \quad (35)$$

$$\overline{\overline{N}} = \epsilon \cos\Delta\hat{\theta} \begin{pmatrix} -1-jx & 1 & 0 & 0 & \cdots & 0 \\ 1 & -2-jx & 1 & 0 & \cdots & 0 \\ 0 & 1 & -2-jx & 1 & \ddots & \vdots \\ \vdots & \ddots & \ddots & \ddots & \ddots & 0 \\ 0 & \cdots & \ddots & 1 & -2-jx & 1 \\ 0 & 0 & \cdots & 0 & 1 & -1-jx \end{pmatrix} \quad (34)$$

By inspection of (34), one can easily see that the term in parentheses, which is the sum of the jth column of $\overline{\overline{N}}$ is simply $-j\omega/\omega_{3\,\mathrm{dB}}$, for all j. Therefore, (35) gives

$$\sum_{j=1}^{N} p_{jk} = \frac{-1}{\dfrac{j\omega}{\omega_{3\,\mathrm{dB}}}}. \tag{36}$$

This is the sum of the kth column of the matrix $\overline{\overline{P}}$ as required for the total noise expression (19), and is exactly the same result that was obtained in the globally coupled system (27). Therefore, the total noise is again given by (28), which implies a noise reduction of $1/N$, independent of the phase difference $\Delta\hat{\theta}$.

The result for the individual oscillator phase fluctuations appears more complicated. Standard matrix methods [17], [18] can be used to evaluate the inverse of (34) for specific numbers of oscillators from which the phase noise can be determined from (14). For example, for $N = 2$:

$$\frac{|\widetilde{\delta\theta}_i|^2_{\Delta\hat{\theta}\neq 0}}{|\widetilde{\delta\theta}_i|^2_{\mathrm{uncoupled}}} = \frac{x^2+2}{x^2+4}. \tag{37}$$

For $N = 3$:

$$\frac{|\widetilde{\delta\theta}_i|^2_{\Delta\hat{\theta}\neq 0}}{|\widetilde{\delta\theta}_i|^2_{\mathrm{uncoupled}}} = \frac{x^4+q_{i1}x^2+3}{x^4+r_{i1}x^2+9}. \tag{38}$$

For $N = 4$:

$$\frac{|\widetilde{\delta\theta}_i|^2_{\Delta\hat{\theta}\neq 0}}{|\widetilde{\delta\theta}_i|^2_{\mathrm{uncoupled}}} = \frac{x^6+q_{i1}x^4+q_{i2}x^2+4}{x^6+r_{i1}x^4+r_{i2}x^2+16} \tag{39}$$

where q_{ij} and r_{ij} are real coefficients. These results can be extrapolated to the general case by induction

$$\frac{|\widetilde{\delta\theta}_i|^2_{\Delta\hat{\theta}\neq 0}}{|\widetilde{\delta\theta}_i|^2_{\mathrm{uncoupled}}} = \frac{x^{2(N-1)}+q_{i,1}x^{2(N-2)}+\cdots+q_{i,N-2}x^2+N}{x^{2(N-1)}+r_{i,1}x^{2(N-2)}+\cdots+r_{i,N-2}x^2+N^2}. \tag{40}$$

Recall that $x = \omega/(\Delta\omega_{\mathrm{lock}}\cos\Delta\hat{\theta})$. Again, the interest is in phase noise near the carrier, in which case the value of $\omega/\Delta\omega_{\mathrm{lock}}$ is very small for most microwave oscillators and coupling configurations. Therefore, as long as $\cos\Delta\hat{\theta} \neq 0$

$$\frac{|\widetilde{\delta\theta}_i|^2_{\Delta\hat{\theta}\neq 0}}{|\widetilde{\delta\theta}_i|^2_{\mathrm{uncoupled}}} \approx \frac{1}{N}. \tag{41}$$

Only when $|\cos\Delta\hat{\theta}| \leq \omega/\Delta\omega_{\mathrm{lock}}$ (i.e., $\Delta\hat{\theta} \approx \pm(\pi/2)$, which corresponds to the maximum stable phase deviation [1]), does the phase noise deviate significantly from the result in (41), at which point

$$\frac{|\widetilde{\delta\theta}_i|^2}{|\widetilde{\delta\theta}_i|^2_{\mathrm{uncoupled}}} \approx 1. \tag{42}$$

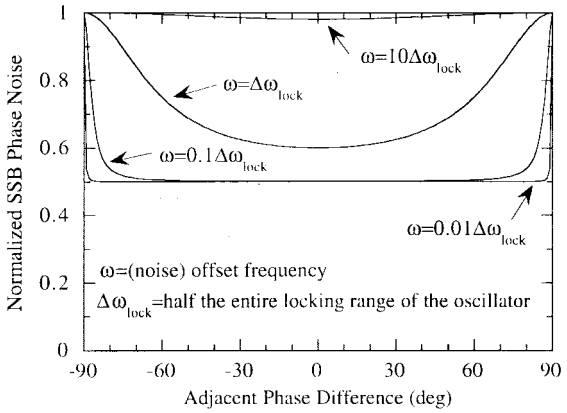

Fig. 3. Individual oscillator phase noise (normalized to an isolated free-running oscillator) versus phase difference between the adjacent oscillators in a two bilaterally coupled oscillator system with $\Phi = 0$. The noise-reduction factor depends both on the phase difference between the oscillators and the frequency offset from the carrier. However, for most systems, the frequency near the carrier $\omega \ll \Delta\omega_{\mathrm{lock}}$ is of most interest where the reduction is $\approx 1/2$ over the entire locking range. Note that this is *not* the total output phase noise, which is *always* reduced by a factor of 1/2 (see text).

This is illustrated in Fig. 3 for a two-oscillator system. The figure shows the phase noise reduction versus oscillator-phase difference for several noise offset frequencies, which are specified with respect to the locking range. As a practical example, noise requirements are often specified in the range of 1–100-kHz offset, whereas a typical number for the locking range in a coupled-oscillator array might be on the order of 100 MHz at X-band. Therefore, the individual oscillator noise reduction can be taken as $1/N$ to a very high degree of accuracy for almost the entire range of allowable phase differences. It should be stressed that Fig. 3 and this discussion are concerned with the noise of a single oscillator in the array and not the total-array output noise, which, as shown previously in (29), is always $1/N$, irrespective of the phase difference and offset frequency.

To summarize, the PM noise of each oscillator is reduced to $1/N$ of its original free-running PM noise within nearly the entire locking range, or equivalently nearly the entire range of allowed phase shift $\Delta\hat{\theta}$. At the locking range edge, the PM noise of each oscillator rapidly returns to its free-running value. The locking effect does not affect each oscillator PM noise outside the locking range.

V. Unilaterally Injection-Locked Oscillators

Another coupling topology that has been reported [3] is the unilaterally injection-locked chain, shown in Fig. 1(c). In this case, each successive oscillator in the chain is slaved to the previous oscillator. The first oscillator in the chain, or *master* oscillator, governs the output frequency and, presumably, the output noise as well. The phase progression can be controlled in this case by manipulating the free-running frequencies of the

individual VCO's. This situation is described by the coupling parameters

$$\epsilon_{ij} = \begin{cases} \epsilon, & i-j=+1 \\ 0, & \text{otherwise} \end{cases}. \tag{43}$$

Assuming the oscillators are all in-phase, the PM noise matrix is given by

$$\overline{\overline{N}} = \epsilon \cdot \begin{pmatrix} -jx & 0 & 0 & \cdots & 0 & 0 \\ 1 & -1-jx & 0 & \cdots & \vdots & \vdots \\ 0 & 1 & -1-jx & \ddots & \vdots & \vdots \\ \vdots & \ddots & \ddots & \ddots & 0 & \vdots \\ 0 & 0 & \ddots & \ddots & -1-jx & 0 \\ 0 & 0 & \cdots & 0 & 1 & -1-jx \end{pmatrix}. \tag{44}$$

This matrix can be inverted analytically to give (45), shown at the bottom of the page, where $x = \omega/\Delta\omega_{\text{lock}}$. Since the rows and columns form geometric series, the sums in (14) and (19) can be evaluated analytically. The resulting expression is complicated for the case of total noise. Approximating for small x, one finds

$$\sum_{i=1}^{N} p_{ij} \approx \begin{cases} \dfrac{-N}{j\epsilon x}, & j=1 \\ -\dfrac{N+1-j}{\epsilon}, & 2 \le j \le N. \end{cases} \tag{46}$$

From (19), the total output phase noise is approximately

$$|\widetilde{\delta\theta}_{\text{total}}|^2 \approx \left[1 + \left(\frac{\omega}{\Delta\omega_{\text{lock}}}\right)^2 \left(\frac{N}{3} - \frac{1}{2} + \frac{1}{6N}\right)\right] \left|\widetilde{\delta\theta}_i\right|^2_{\text{uncoupled}}. \tag{47}$$

So there is a slight noise degradation which increases quadratically away from the carrier, and linearly with increasing array length. For most arrays this would be a small effect since the near-carrier noise is of most concern, for which $\omega/\Delta\omega_{\text{lock}} \ll 1$. At the carrier frequency, the noise is just that of the first-stage oscillator. The total noise could be significantly reduced by making the first-stage oscillator a low-noise source.

The phase noise of the individual oscillators in the array can be evaluated without approximation to give

$$|\widetilde{\delta\theta}_i|^2 = |\widetilde{\delta\theta}_i|^2_{\text{uncoupled}}. \tag{48}$$

Therefore, one can conclude that the unilateral injection locking does not improve the phase noise for the total array or the individual elements in the array. A low phase noise in this case can only be obtained by a low-noise master oscillator.

VI. General Results for Reciprocal Coupling Networks

The previous sections illustrated the importance of the coupling network in determining the noise fluctuations in the oscillator array. The interesting fact that both the globally coupled array and the nearest-neighbor coupling network both lead to a $1/N$ reduction in the total phase noise suggests that this may be a property of reciprocal coupling networks in general, and not merely a special case. This will be proven in this section.

When the oscillators are described by parallel-resonator equivalent circuits, it has been shown in [13] that it is most appropriate to describe the N-port coupling network in terms of admittance parameters Y_{ij} (Fig. 4). The normalized coupling coefficients in this case are given by

$$\kappa_{ij} = \frac{Y_{ij}}{G_L} = \epsilon_{ij} e^{-j\Phi_{ij}} \tag{49}$$

where G_L, ϵ_{ij}, and Φ_{ij} are the oscillator output load admittance, the magnitude of coupling coefficient, and the coupling phase.

Assuming that the N-port coupling network is composed of linear time-invariant elements (resistors, capacitors, inductors, transmission lines, etc.), the coupling network is reciprocal such that [6]

$$Y_{ij}(j\omega) = Y_{ji}(j\omega). \tag{50}$$

$$\overline{\overline{P}} = \frac{1}{\epsilon} \begin{pmatrix} \dfrac{-1}{jx} & 0 & 0 & \cdots & 0 & 0 \\ \dfrac{-1}{jx(1+jx)} & \dfrac{-1}{1+jx} & 0 & \cdots & 0 & 0 \\ \dfrac{-1}{jx(1+jx)^2} & \dfrac{-1}{(1+jx)^2} & \dfrac{-1}{1+jx} & \ddots & \vdots & 0 \\ \vdots & \vdots & \vdots & \ddots & 0 & \vdots \\ \dfrac{-1}{jx(1+jx)^{N-2}} & \dfrac{-1}{(1+jx)^{N-2}} & \dfrac{-1}{(1+jx)^{N-3}} & \cdots & \dfrac{-1}{1+jx} & 0 \\ \dfrac{-1}{jx(1+jx)^{N-1}} & \dfrac{-1}{(1+jx)^{N-1}} & \dfrac{-1}{(1+jx)^{N-2}} & \cdots & \dfrac{-1}{(1+jx)^2} & \dfrac{-1}{1+jx} \end{pmatrix} \tag{45}$$

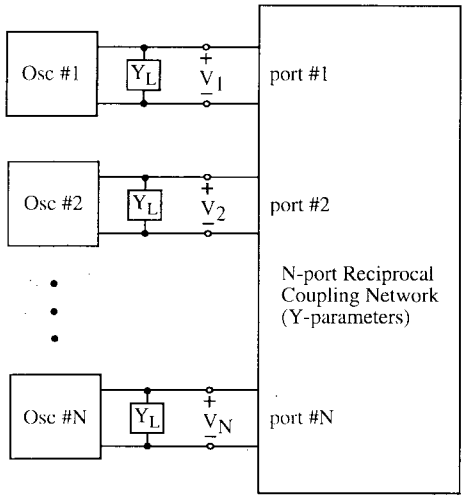

Fig. 4. The N-port reciprocal coupling network.

Therefore, a reciprocal coupling network requires that

$$\epsilon_{ij} = \epsilon_{ji}. \tag{51}$$

For N-coupled oscillators with $\Phi_{ij} = 0$ (or some multiple of 2π), the elements of matrix $\overline{\overline{N}}$ from (9) are

$$n_{ij} = \begin{cases} -\jmath\left(\dfrac{\omega}{\omega_{3\,\mathrm{dB}}}\right) - \displaystyle\sum_{j=1}^{N} \epsilon_{ij} \cos(\hat{\theta}_i - \hat{\theta}_j), & i = j \\ \epsilon_{ij} \cos(\hat{\theta}_i - \hat{\theta}_j), & i \neq j. \end{cases} \tag{52}$$

If the coupling network is reciprocal, then from (51) one can see that $n_{ij} = n_{ji}$, and from (52) one has

$$\sum_{i=1}^{N} n_{ij} = \sum_{j=1}^{N} n_{ij} = -\jmath\left(\frac{\omega}{\omega_{3\,\mathrm{dB}}}\right). \tag{53}$$

Therefore, using (35) gives

$$\sum_{i=1}^{N} p_{ij} = \frac{-1}{\dfrac{\jmath\omega}{\omega_{3\,\mathrm{dB}}}} \tag{54}$$

and substituting into (19), the total phase noise of N reciprocally coupled oscillators is

$$|\widetilde{\delta\theta}_{\mathrm{total}}|^2 = \frac{1}{N} \left|\widetilde{\delta\theta}_i\right|^2_{\mathrm{uncoupled}}. \tag{55}$$

Therefore, the total PM noise of N oscillators coupled through an *arbitrary* reciprocal coupling network always leads to a $1/N$ reduction in the total phase noise. This is a useful result which applies to two-dimensional (2-D) arrays, coupling loops, and other structures satisfying the reciprocity condition (50).

VII. Phase Noise of Coupled Oscillators with Small Nonzero Coupling Phase Φ

In the previous sections one has assumed that the coupling phase was adjusted so that $\Phi = 0$. In practice, it is difficult to achieve this exactly. In this section, one will attempt to study the effect of nonzero Φ. From (4) with nonzero Φ_{ij}, assuming identical oscillator amplitudes (12), and neglecting the AM-to-PM noise conversion, the elements of the coupling matrix $\overline{\overline{N}}$ are found to be

$$n_{ij} = \begin{cases} -\jmath\left(\dfrac{\omega}{\omega_{3\,\mathrm{dB}}}\right) - \displaystyle\sum_{j=1}^{N} \epsilon_{ij} \cos(\hat{\theta}_i - \hat{\theta}_j) \cos\Phi_{ij} \\ \quad + \displaystyle\sum_{j=1}^{N} \epsilon_{ij} \sin(\hat{\theta}_i - \hat{\theta}_j) \sin\Phi_{ij}, & i = j \\ \epsilon_{ij} \cos(\hat{\theta}_i - \hat{\theta}_j) \cos\Phi_{ij} - \epsilon_{ij} \sin(\hat{\theta}_i - \hat{\theta}_j) \\ \quad \cdot \sin\Phi_{ij}, & i \neq j. \end{cases} \tag{56}$$

The coupling network is assumed reciprocal (i.e., $\epsilon_{ij} = \epsilon_{ji}$). It has been shown [1] that the free-running frequencies in the array can always be chosen to establish the in-phase condition (i.e., $\Delta\hat{\theta} = 0$), even when the coupling phase is nonzero. For this particular phase distribution, $n_{ij} = n_{ji}$ and

$$\sum_{i=1}^{N} n_{ij} = -\jmath\left(\frac{\omega}{\omega_{3\,\mathrm{dB}}}\right). \tag{57}$$

From (35), the coupled oscillator array has the same properties as the array with $\Phi_{ij} = 0$ (or 2π)

$$|\widetilde{\delta\theta}_{\mathrm{total}}|^2 = \frac{1}{N} \left|\widetilde{\delta\theta}_i\right|^2_{\mathrm{uncoupled}}. \tag{58}$$

However, when the adjacent phase difference between the oscillators is nonzero, then the coupling matrix is no longer symmetrical ($n_{ij} \neq n_{ji}$). Therefore, the results of the previous section no longer apply, and the noise properties of the array will deviate from that predicted by (58). Unfortunately, the matrix $\overline{\overline{N}}$ can no longer be inverted analytically in the general case, and, in fact, is difficult to do even for small arrays. The two-oscillator system will be examined in an effort to determine the qualitative behavior of the arrays for nonzero Φ.

Following the procedures established in the previous sections, the total phase noise for two mutually coupled oscillators, using the coupling matrix in (56), becomes

$$\frac{|\widetilde{\delta\theta}_{\mathrm{total}}|^2}{|\widetilde{\delta\theta}_i|^2_{\mathrm{uncoupled}}} = \frac{1}{2} \frac{\left(\dfrac{\omega}{\Delta\omega_{\mathrm{lock}}}\right)^2 + 2[\cos^2(\Delta\hat{\theta} + \Phi) + \cos^2(-\Delta\hat{\theta} + \Phi)]}{\left(\dfrac{\omega}{\Delta\omega_{\mathrm{lock}}}\right)^2 + [\cos(\Delta\hat{\theta} + \Phi) + \cos(-\Delta\hat{\theta} + \Phi)]^2}. \tag{59}$$

This expression is plotted in Fig. 5 at a fixed coupling phase of $\Phi = 10°$, for several different offset frequencies, versus the phase difference between the two oscillators. Close to the carrier, the total noise peaks dramatically at the edges of the locking range, but approaches a finite value depending

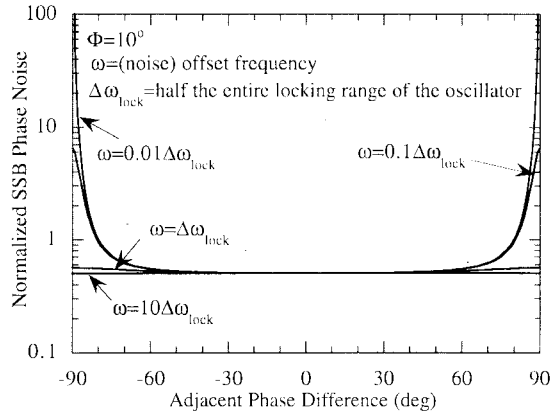

Fig. 5. Total phase noise (normalized to an isolated free-running oscillator) versus phase difference between the adjacent oscillators in a two bilaterally coupled oscillator system with $\Phi = 10°$. Close to the carrier, the total noise peaks dramatically at the edges of the locking range, but approaches a finite value depending on the magnitude of the coupling phase and the offset from the carrier. Far from the carrier, the noise is not significantly affected by the coupling phase, and a noise reduction of one-half is observed over nearly the entire locking range.

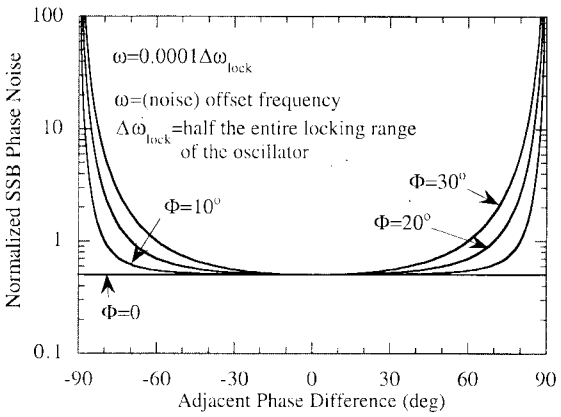

Fig. 6. Total phase noise (normalized to an isolated free-running oscillator) versus phase difference between the adjacent oscillators in a two bilaterally coupled oscillator system for a number of different coupling phases at one particular offset frequency close to the carrier. The total noise peaks dramatically at the edges of the locking range when Φ deviates from zero. As Φ is close to zero, the total phase noise is not significantly affected by the coupling phase, and a noise reduction of one-half is observed over nearly the entire locking range.

on the magnitude of the coupling phase and the offset from the carrier. Far from the carrier, the noise is not significantly affected by the coupling phase, and a noise reduction of 1/2 is observed over nearly the entire locking range. Similarly, Fig. 6 shows the total noise versus phase difference for a number of different coupling phases at one particular offset frequency.

The general behavior exhibited in Figs. 5 and 6 are expected to hold for large arrays, at least qualitatively. One complication, however, is that the range of allowed (stable) phase shifts depends strongly on the coupling phase Φ and the number of the oscillators, and is no longer $-90° < \Delta\hat{\theta} < +90°$ in general. Therefore, a numerical computation of array noise must first involve finding solutions to the dynamic equations (2) for a given set of free-running frequencies, deciding which of these is stable, and then computing the inverse coupling matrix $\overline{\overline{P}}$ to determine the noise properties.

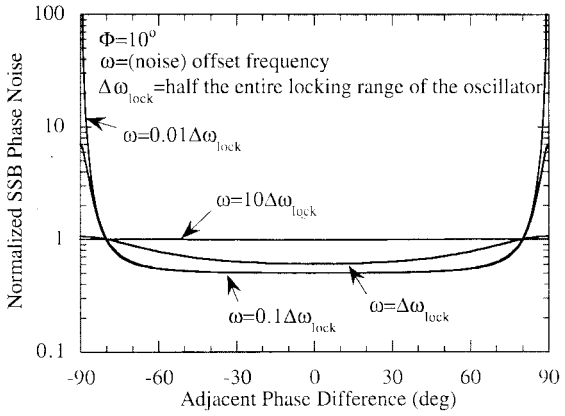

Fig. 7. Individual oscillator phase noise (normalized to an isolated free-running oscillator) versus phase difference between the adjacent oscillators in a two bilaterally coupled oscillator system with $\Phi = 10°$. Near the carrier ($\omega \ll \Delta\omega_{\text{lock}}$), the individual noise shows a reduction of one-half near the center of the locking range, and increasing dramatically near the locking band edge. Far from the carrier (i.e., $\omega \gg \Delta\omega_{\text{lock}}$) the individual noise spectrum returns to its free-running value.

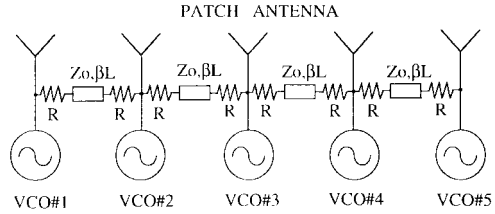

Fig. 8. Diagram of five-element coupled oscillator array.

The noise property of the individual oscillators in the two mutually coupled oscillators with $\Phi \neq 0$ is also of interest. The individual oscillator phase noise is found as

$$\frac{|\widetilde{\delta\theta}_i|^2}{|\widetilde{\delta\theta}_i|^2_{\text{uncoupled}}} = \frac{\left(\dfrac{\omega}{\Delta\omega_{\text{lock}}}\right)^2 + [\cos^2(\Delta\hat{\theta}+\Phi) + \cos^2(-\Delta\hat{\theta}+\Phi)]}{\left(\dfrac{\omega}{\Delta\omega_{\text{lock}}}\right)^2 + [\cos(\Delta\hat{\theta}+\Phi) + \cos(-\Delta\hat{\theta}+\Phi)]^2}. \tag{60}$$

This expression is plotted in Fig. 7 for $\Phi = 10°$, for a range of offset frequencies. Near the carrier ($\omega \ll \Delta\omega_{\text{lock}}$), the individual noise is identical to that of (59), showing a reduction of one-half near the center of the locking range, and increasing dramatically near the locking band edge. Far from the carrier (i.e., $\omega \gg \Delta\omega_{\text{lock}}$) the individual noise spectra returns to its free-running value.

VIII. Experimental Results for Nearest-Neighbor Coupling

A five-element linear coupled oscillator chain was built for experimental verification of the theory for a bilaterally coupled array. This is shown in Fig. 8, and is a similar design to previously reported work by the authors [13]. The array is composed

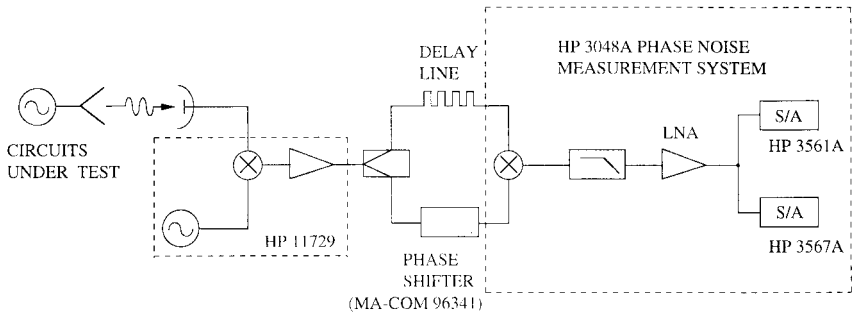

Fig. 9. Phase noise measurement setup using a frequency discriminator method.

of five varactor-tuned MESFET VCO's with a nominal tuning range of 8.0–9.0 GHz. These VCO's use NE32184A packaged MESFET's and MA-COM 46 600 varactor diodes. The VCO's are coupled together by a one-wavelength (at about 8.5-GHz) microstrip transmission lines and are resistively loaded with two 75-Ω chip resistors as shown in Fig. 8. As described in [13], this technique provides coupling parameters $\epsilon \approx 0.5$ and $\Phi = \beta L \approx 2\pi$. Each oscillator is designed to deliver power to a 50-Ω load. The oscillators were "connectorized" using SMA-to-microstrip transitions, which allowed for simple testing, and later, connection to an external five-element patch antenna array.

As described in [2], varying the end-element free-running frequencies induces a constant phase progression along the array. Representative radiation patterns for the experimental array for various end-element detunings are found in [2], [4]. When all elements are set to a common free-running frequency, the elements are nominally in phase and a broadside beam is expected. It was found that the array can remain locked within a maximum end-element detuning of approximately ± 125 MHz, which gives an estimation of the locking range.

Because of VCO's inherent poor phase noise behavior and comparatively large thermal drift, a frequency discriminator technique was used for the phase noise measurement. This experimental apparatus is illustrated in Fig. 9. The frequency discriminator is implemented with a delay line and a phase detector. Due to the high insertion loss of the delay line at microwave frequencies, the signal to be measured was first downconverted to a $\sim$1.0-GHz intermediate frequency. The source acting as the local oscillator has at least 40-dB lower phase noise than the signal to be tested, so its phase noise contribution to the final measurement result can be neglected. The down-converted signal is amplified by a power amplifier and split into two channels. The signal in one channel is delayed relative to the other. The unequal delay converts the frequency fluctuation in the signal under test to a phase fluctuation. Determination of the delay time involves a tradeoff among the noise floor, offset frequency, and the tolerable insertion loss. In this case, a 23.0-ns delay time was chosen, giving a noise floor at least 40-dB lower than the expected phase noise of the signal under test up to approximately a 6-MHz offset frequency. In the other channel, a phase shifter is used to maintain quadrature between the signals in these two channels.

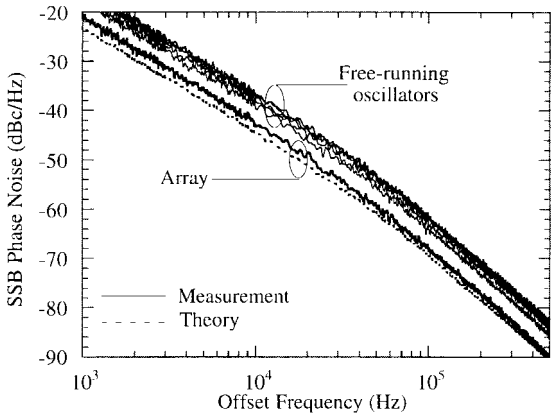

Fig. 10. Comparison of the free-running PM noise for each of the five oscillators in the experimental array with the total PM noise measured in the far field. The theoretical noise reduction is shown for comparison, which is the average free-running noise divided by five.

This apparatus was used to characterize both the total output array noise and the individual oscillator fluctuations in a variety of conditions. For total array noise, the oscillators were connected to a patch antenna array and the output signal was measured with a detector in the far field. Isolators were placed between the oscillator output and the antenna feed to maintain a 50-Ω load impedance. For the individual oscillator measurements, the oscillators were connected directly to the measurement system using SMA cables. Fig. 10 shows that the phase noise of the individual array elements when free-running, and the total array output under synchronized conditions (all oscillators set to a common free-running frequency). The total output phase noise is clearly reduced as compared to those of the free-running oscillators. In this and all subsequent figures, the noise in the range of offset frequencies from 1 kHz to 0.5 MHz is shown, which is a range of common interest.

The theoretical result using (29) is shown for comparison, and shows close agreement to the measurements. The small difference between the measurement and theoretical values could be due to a number of influences that are neglected in this analysis, including the assumption of the nearest neighbor coupling, the approximation for total output phase noise (19), possibly small nonzero coupling phase ($\Phi_{ij} \neq 0$), and the neglect of transformation of amplitude noise to phase noise.

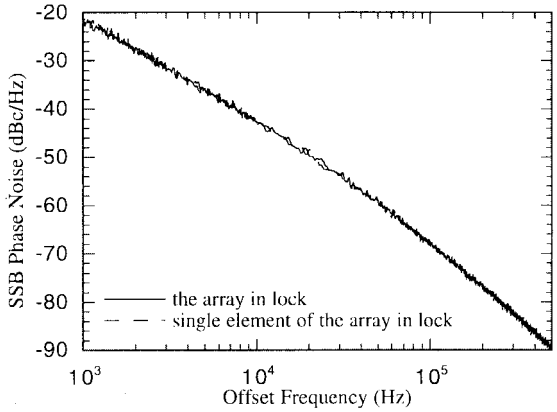

Fig. 11. Phase noise of the array output and single oscillator under locked conditions.

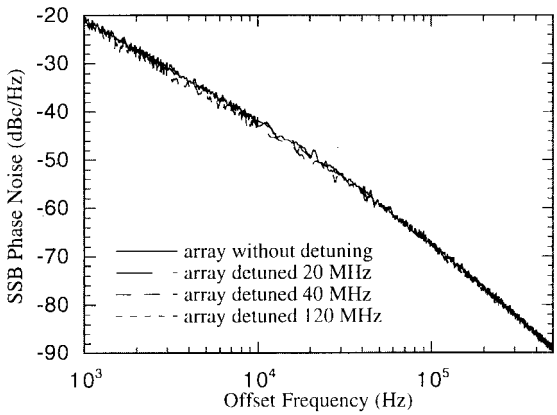

Fig. 12. The total phase noise of the array with and without detuning of both end oscillators. The graph confirms that inter-element phase shift does not significantly change the phase noise-reduction factor.

Fig. 11 shows that the phase noise of the individual oscillator in the array, under locked conditions, is also reduced by the same factor as the array. This agrees with the prediction of (41), which is expected here since the range of offset frequencies is much smaller than the locking range by orders of magnitude.

The previous two figures are for the special case of in-phase (or nearly in-phase) operation of the array elements. The nonzero phase progression can be established by detuning the end-elements in the array. The influence of this progressive phase shift on the total output noise is shown in Fig. 12, and confirms again the theoretical prediction that the noise reduction factor is independent of the phase difference, within experimental uncertainty, over much of the allowable range of phase shifts.

IX. Conclusions

Analysis of phase noise near the carrier in coupled-oscillator arrays with parallel resonator model and $\Phi = 0$ has been analyzed for a few common coupling topologies, and a reduction proportional to the number of oscillators is found in each case. The total phase noise of N bilaterally reciprocal coupled oscillators with $\Phi = 0$ also shows the reduction of $1/N$ without using the assumption of nearest-neighbor coupling. Such general results can cover any arbitrary coupling circuit, such as the bilaterally coupled loop and 2-D coupled oscillators. The effect of small nonzero coupling phase Φ on the phase noise of the array and individual oscillator is studied and the phase noise deteriorates as the adjacent phase difference between oscillators approaches the locking range edge. Measurements for a small MESFET oscillator array at X-band confirm the noise reduction.

This paper has neglected the influence of AM noise, which will affect the PM results in the case of a nonzero phase progression. Furthermore, AM noise does not necessarily decrease with increasing numbers of oscillators [16] and, therefore, must be examined to determine possible limitations on array size. The analysis presented here also neglects possible correlations between the oscillator noise sources, and the influence of nonuniform amplitude and phase distributions, but these are thought to be minor effects in a practical sense. Although the general case involving arbitrary arrays and frequency distributions is impossible to treat analytically, it can be treated computationally using the dynamic equations described at the beginning of the paper. This will probably be necessary for 2-D arrays of oscillators [19], even for simple topologies, due to the mathematical complexity of the coupling matrix.

Acknowledgment

The authors wish to thank the NEC Company for donating the MESFET devices and the Rogers Company for donating the Duroid boards.

References

[1] R. A. York, "Nonlinear analysis of phase relationships in quasi-optical oscillator arrays," *IEEE Trans. Microwave Theory Tech.*, vol. 41, pp. 1799–1809, Oct. 1993.
[2] P. Liao and R. A. York, "A new phase-shifterless beam scanning technique using arrays of coupled oscillators," *IEEE Trans. Microwave Theory Tech.*, vol. 41, pp. 1810–1815, Oct. 1993.
[3] S. T. Chew, T. K. Tong, M. C. Wu, and T. Itoh, "An active phased array with optical input and beam-scanning capability," *IEEE Microwave Guided Wave Lett.*, vol. 3, pp. 347–349, Oct. 1994.
[4] X. Cao and R. A. York, "Phase noise reduction in scanning oscillator arrays," in *IEEE MTT-S Int. Microwave Symp. Dig.*, Orlando, FL, 1995, pp. 769–772.
[5] W. R. Braun, "Short term frequency instability effects in networks of coupled oscillators," *IEEE Trans. Commun.*, vol. COM-28, pp. 1269–1275, Aug. 1980.
[6] L. O. Chua, C. A. Desoer, and E. S. Kuh, *Linear and Nonlinear Circuits*, 1st ed. New York: McGraw-Hill, 1987.
[7] J. G. Proakis, *Digital Communications*, 2nd ed. New York: McGraw-Hill, 1989.
[8] Y. Okabe and S. Okamura, "Analysis of the stability and noise of oscillators in free, synchronized, and parallel running modes," *Elect. Commun. Jap.*, vol. 52-B, no. 12, pp. 102–110, 1969.
[9] ——, "Stability and noise of many oscillators in parallel running," *Elect. Commun. Jap.*, vol. 53-B, no. 12, pp. 94–103, 1970.
[10] T. Makino, M. Nakajima, and J. Ikenoue, "Noise reduction mechanism of a power combining oscillator system," *Elect. Commun. Jap.*, vol. 62-B, no. 4, pp. 37–44, 1979.
[11] H. Stark and J. W. Woods, *Probability, Random Processes, and Estimation Theory for Engineers*. New York: Prentice-Hall, 1986.
[12] S. Hamilton, "FM and AM noise in microwave oscillators," *Microwave J.*, vol. 21, pp. 105–109, June 1978.
[13] R. A. York, P. Liao, and J. J. Lynch, "Oscillator array dynamics with broad-band N-port coupling networks," *IEEE Trans. Microwave Theory Tech.*, vol. 42, pp. 2040–2045, Nov. 1994.

[14] K. Kurokawa, "The single-cavity multiple-device oscillator," *IEEE Trans. Microwave Theory Tech.*, vol. MTT-19, pp. 793–801, Oct. 1971.
[15] _____, "Noise in synchronized oscillators," *IEEE Trans. Microwave Theory Tech.*, pp. 234–240, Apr. 1968.
[16] W. O. Schlosser, "Noise in mutually synchronized oscillators," *IEEE Trans. Microwave Theory Tech.*, vol. MTT-16, pp. 732–737, Sept. 1968.
[17] R. A. Usmani, "Bounds for the solution of a second order differential equation with mixed boundary conditions," *J. Eng. Math.*, vol. 9, no. 2, pp. 159–164, Apr. 1975.
[18] C. F. Fischer and R. A. Usmani, "Properties of some tridiagonal matrices and their application to boundary value problems," *SIAM J. Numer. Anal.*, vol. 6, no. 1, pp. 127–142, Mar. 1969.
[19] J. B. Hacker, M. P. De Lisio, M. Kim, C.-M. Liu, S.-J. Li, S. W. Wedge, and D. B. Rutledge, "A 10-watt X-band grid oscillator," in *IEEE MTT-S Int. Microwave Symp. Dig.*, San Diego, CA, 1994, pp. 823–826.

Heng-Chia Chang received the B.S. degree in electrical engineering from National Taiwan University, Taipei, Taiwan, in 1990, and M.S. degree from the University of California at Santa Barbara, in 1994. He is currently working toward the Ph.D. degree at the University of California at Santa Barbara.

From 1990 to 1992, he served in the Air Force as a Technical Officer in Taiwan. He also received maintenance training about various wireless communication systems, GCA radar, digital fiber-optical communication systems, and digital PABX system. His current research interests include noise analysis, nonlinear microwave circuit design, coupled oscillator theory, nonlinear optics, and statistical optics.

Xudong Cao received the B.S.E.E. degree from the Beijing University of Aeronautics, Beijing, China, in 1982.

He is presently a Senior Engineer at Luoyang Optical and Electrical Institute (LOEI), Henan, China. He has worked as a Visiting Researcher at the University of California at Santa Barbara, since 1994. Since joining LOEI in 1982, he has been involved in the design of several microwave and millimeter-wave sources. Currently he is engaged in the development of the low-phase noise frequency agile source. His research interests are in the phase noise reduction technique, noise theory of solid-state oscillators and devices, low-frequency noise measurement, and low-frequency noise in GaAs MESFET's.

Umesh K. Mishra (S'80–M'83–SM'90–F'95) received the B.Tech. degree from the Indian Institute of Technology, Kanpur, India, the M.S. degree from Lehigh University, Bethlehem, PA, and the Ph.D. degree from Cornell University, Ithaca, NY, all in electrical engineering, in 1979, 1981, and 1984, respectively.

From 1983 to 1985, he was a Process Engineer at General Electric Company, Syracuse, NY. From 1985 to 1986, he was an Assistant Professor in the Department of Electrical Engineering and Computer Science, University of Michigan, Ann Arbor. He was the Principal Staff Engineer at General Electric Company and IEEE-MIT National Lecturer of Speakers Bureau, in 1985 and 1988, respectively. In 1988, he was with Hughes Research Laboratories as a Member of the Technical Staff. From 1989 to 1990, he was an Associate Professor at North Carolina State University. He joined the faculty of the University of California at Santa Barbara in 1991, where he is currently a Professor. His current research interests include semiconductor device physics, quantum electronics design and fabrication, optical control of microwave and millimeter-wave devices, nanometer fabrication techniques, *in situ* processing, and integration techniques.

In 1995, Dr. Mishra was awarded the Gledden Visiting Senior Fellowship from the University of Western Australia, Australia. He was awarded the Junior Science Talent Scholarship, the National Science Talent Search Scholarship from the Government of India, the Best Project Award in electrical engineering for his B.Tech. thesis, and the Sherman Fairchild Fellowship from Lehigh University, in 1972, 1974, 1979, and 1980, respectively. In 1989 and 1990, he was awarded the Presidential Young Investigator Award and the Young Scientist of the Year Award (International GaAs Symposium).

Robert A. York (S'85–M'89) received the B.S. degree in electrical engineering from the University of New Hampshire, Durham, and the M.S. and Ph.D. degrees in electrical engineering from Cornell University, Ithaca, NY, in 1987, 1989, and 1991, respectively.

He is currently an Associate Professor of Electrical and Computer Engineering at the University of California at Santa Barbara. His group at the University of California at Santa Barbara is currently involved with the design and fabrication of microwave and millimeter-wave circuits, microwave photonics, high-power microwave and millimeter-wave modules using spatial combining and wide-bandgap semiconductor devices, and time-domain modeling of antennas, power-combining arrays, and other electromagnetic or electronic structures.

Dr. York received the Army Research Office Young Investigator Award in 1993 and the Office of Naval Research Young Investigator Award in 1996.